Published in "Journal of Biological Chemistry 280(23): 22515-22522, 2005"
which should be cited to reference this work.

Synthesis of Sphingolipids with Very Long Chain Fatty Acids but Not Ergosterol Is Required for Routing of Newly Synthesized Plasma Membrane ATPase to the Cell Surface of Yeast*

Barbara Gaigg, Birgit Timischl, Linda Corbino, and Roger Schneiter‡

From the Division of Biochemistry, University of Fribourg, CH-1700 Fribourg, Switzerland

The proton pumping H^+-ATPase, Pma1p, is an abundant and very long-lived polytopic protein of the *Saccharomyces cerevisiae* plasma membrane. Pma1p constitutes a major cargo of the secretory pathway and thus serves as an excellent model to study plasma membrane biogenesis. We have previously shown that newly synthesized Pma1p is mistargeted to the vacuole in an *elo3*Δ mutant that affects the synthesis of the ceramide-bound C26 very long chain fatty acid (Eisenkolb, M., Zenzmaier, C., Leitner, E., and Schneiter, R. (2002) *Mol. Biol. Cell* 13, 4414–4428) and now describe a more detailed analysis of the role of lipids in Pma1p biogenesis. Remarkably, a block at various steps of sterol biosynthesis, a complete block in sterol synthesis, or the substitution of internally synthesized ergosterol by externally supplied ergosterol or even by cholesterol does not affect Pma1p biogenesis or its association with detergent-resistant membrane domains (lipid "rafts"). However, a block in sphingolipid synthesis or any perturbation in the synthesis of the ceramide-bound C26 very long chain fatty acid results in mistargeting of newly synthesized Pma1p to the vacuole. Mistargeting correlates with a lack of newly synthesized Pma1p to acquire detergent resistance, suggesting that sphingolipids with very long acyl chains affect sorting of Pma1p to the cell surface.

Integral membrane proteins destined to the cell surface enter the membrane in the ER[1] and are then transported along the secretory pathway to the plasma membrane. Along this route, the quality of the transported cargo is monitored at several steps to ensure that only functional proteins are delivered to the cell surface. Surface delivery of membrane proteins is likely coupled to expansion of the plasma membrane itself, implying that transport and sorting of proteins may be linked to that of lipids. Whereas the mechanisms that survey protein sorting and quality control are being studied intensively, the fate of lipids along this route and their possible roles in protein sorting and maturation are less well understood (1, 2).

The proton pumping H^+-ATPase, Pma1p, is an abundant and long-lived polytopic membrane protein of the yeast plasma membrane. Due to its abundance at the cell surface, Pma1p constitutes a major cargo of the secretory pathway and thus may serve as a model to study plasma membrane biogenesis (3, 4). Pma1p is biosynthetically inserted into the ER membrane, where it homo-oligomerizes to form a 1.8-MDa complex that resists extraction by detergents (5). This protein-lipid complex is then packaged into a larger subclass of COPII transport vesicles that contain Lst1p instead of Sec24p (6). From the Golgi complex, Pma1p is transported to the cell surface by a branch of the secretory pathway that does not intersect with endosomes (7, 8). At the cell surface, Pma1p becomes stabilized and occupies domains that are distinct from those occupied by the arginine/H^+ symporter Can1p (9).

Similar to the synthesis of integral membrane proteins, the synthesis of sphingolipids commences in the ER, where serine palmitoyl transferase catalyzes the condensation of serine with palmitoyl-CoA to form a long chain base. The long chain base then condenses with a C26 very long chain fatty acid to form ceramide in a reaction that requires *LAG1*, *LAC1*, and *LIP1* (10–12). From the ER, ceramide is transported both by vesicular and non-vesicular routes to the Golgi, where it is converted to sphingolipids (13, 14). Mature sphingolipids are then transported to the plasma membrane, where they are highly enriched (15–17).

The ceramide-bound C26 very long acyl chain is synthesized by elongation of saturated long chain fatty acids by an ER-associated acyl chain elongation complex containing Elo2p/Fen1p, Elo3p/Sur4p, Tsc13p, Ybr159p, and soluble factors such as palmitoyl-CoA (Acb1p) and malonyl-CoA (synthesized by Acc1p), which provide the substrates for elongation (18–22). The physiological significance of the very long chain fatty acid substitution on the fungal ceramide is unknown, but it has been speculated that the length of the transmembrane domain of proteins along the secretory pathway may increase to match bilayers of increasing "thickness" (14). In such a model, the abundance of C26-containing lipids may determine the thickness of membranes along the secretory pathway.

A relationship between Pma1p biogenesis and lipid synthesis is indicated by a number of observations. Long chain base or ceramide synthesis is required for oligomerization and raft association of Pma1p in the ER (5, 23). Oligomerization of Pma1p, however, is not required for ER export or surface delivery but might be important for stabilization of the protein once it has reached the cell surface (5, 23). In addition, raft association of Pma1p is important for its proper surface targeting and for the subsequent stabilization of the protein at the cell surface (23–25).

We have previously observed that newly synthesized Pma1p is mistargeted to the vacuole in a mutant that affects acyl chain elongation and hence C26 synthesis (*elo3*/*sur4*) (26). The aim of the present study was to characterize the role of lipids and

* This work was supported by Grant 631-065925 from the Swiss National Science Foundation. The costs of publication of this article were defrayed in part by the payment of page charges. This article must therefore be hereby marked "*advertisement*" in accordance with 18 U.S.C. Section 1734 solely to indicate this fact.

‡ To whom correspondence should be addressed: Dept. of Medicine, Division of Biochemistry, University of Fribourg, Chemin du Musée 5, CH-1700 Fribourg, Switzerland. Tel.: 41-26-300-8654; Fax: 41-26-300-9735; E-mail: roger.schneiter@unifr.ch.

[1] The abbreviations used are: ER, endoplasmic reticulum; ALA, δ-aminolevulinic acid; IPC, inositolphosphorylceramide; GFP, green fluorescent protein.

TABLE I
S. cerevisiae strains used in this study

Strain	Relevant genotype	Source
BY4742	*MATα his3Δ1 leu2Δ0 ura3Δ0 lys2Δ0*	EUROSCARF (27)
	MATα his3Δ1 leu2Δ0 ura3Δ0 lys2Δ0 xyz::kanMX	EUROSCARF (27); *xyz* indicates a deletion in a nonessential gene used in this study
RH2607	*MAT***a** *his4 leu2 ura3 bar1 lcb1–100*	H. Riezman (33)
YRS1593	*MAT***a** *leu2 ura3 lys2 trp1 tsc13^{ts}*	T. Dunn (19)
YRS1041	*MAT***a** *ade2–101 ura3–52 leu2-Δ1 lys2–801 acc1^{ts}*	Ref. 22
YRS1550	*MATα his3Δ1 leu2Δ0 ura3Δ0 lys2Δ0 elo3::his5MX6 pep4::LEU2*	Ref. 26
YRS1707	*MATα his3Δ1 leu2Δ0 ura3Δ0 lys2Δ0 hem1::LEU2*	This study
YRS1714	*MATα his3Δ1 leu2Δ0 ura3Δ0 lys2Δ0 elo2::kanMX4 pep4::LEU2*	This study
YRS1546	*MAT? his3Δ200 leu2Δ1 ura3–52 trp1Δ63 pep4::URA3*	This study
YRS1718	*MATα his3Δ1 leu2Δ0 ura3Δ0 lys2Δ0 acb1::kanMX4 pep4::LEU2*	This study
YRS1716	*MAT***a** *leu2 ura3 lys2 trp1 tsc13–1 pep4::LEU2*	This study
YRS1917	*MAT***a** *ade2–101 ura3–52 leu2-Δ1 lys2–801 acc1^{ts} pep4::LEU2*	This study
YRS1986	*MAT***a** *his4 leu2 ura3 bar1 lcb1–100 elo3::kanMX4*	This study
YRS1825	*MATα his3Δ1 leu2Δ0 lys2Δ0 ura3Δ0 are1::kanMX4 are2::HIS3MX6*	This study

particularly that of the C26 very long chain fatty acid in surface transport of Pma1p in more detail. Pulse-chase analyses to follow Pma1p biogenesis in various lipid biosynthetic mutants indicate that any reduction in the efficiency of the fatty acid elongation pathway results in destabilization of newly synthesized Pma1p. These results suggest that ceramide levels and/or their substitution with saturated very long chain fatty acids is important for proper routing of Pma1p to the cell surface.

EXPERIMENTAL PROCEDURES

Yeast Strains and Growth Conditions—Yeast strains used in this study are listed in Table I. Strains bearing single deletions of nonessential genes were obtained from EUROSCARF (see www.rz.uni-frankfurt.de/FB/fb16/mikro/euroscarf/index.html) (27). Strains were cultivated at 24 °C, 30 °C, or 37 °C in YPD-rich media (1% Bacto yeast extract, 2% Bacto peptone (USBiological, Swampscott, MA), 2% glucose) or in minimal media. Selection for the kanMX marker was on media containing 200 μg/ml G418 (Invitrogen). Unless otherwise noted, chemicals were purchased from Sigma. Aureobasidin A was obtained from Takara Bio Inc. (Shiga, Japan), myriocin and fumonisin B1 were from Alexis Corp. (Lausen, Switzerland), and terbinafine was a kind gift from N. Ryder (Novartis Research Institute, Vienna, Austria). Media supplemented with sterols contained 5 mg/ml Tween 80 and 20 μg/ml ergosterol or cholesterol. *hem1*Δ mutant cells were supplemented with 10 μg/ml δ-aminolevulinic acid (ALA).

For DNA cloning and propagation of plasmids, *Escherichia coli* strain XL1-blue (Stratagene) was used. To generate double mutants with *pep4*Δ, a *pep4*::*LEU2* disruption cassette (pTS17; Tom Stevens, University of Oregon, Eugene, OR) was cut with BamHI and used for transformation of elongase mutants. *PEP4* disruption was confirmed by PCR and a plate assay for carboxypeptidase Y activity. To generate the *hem1*Δ mutant, the plasmid pHEM1-LEU2 containing the *hem1*::*LEU2* disruption cassette (kindly provided by I. Hapala, Slovak Academy of Sciences, Bratislava, Slovak Republic) was cut with BamHI/HindIII to release the disruption cassette, and transformants were selected on minimal media without leucine but supplemented with ALA. Correct insertion of the disruption cassette at the *HEM1* locus was confirmed by phenotypic analysis, *i.e.* growth on ALA-supplemented media, but no growth on non-supplemented media. The plasmid containing a GFP-tagged version of Pma1p was kindly provided by A. Breton (Institut de Biochimie et Genetique Cellulaires, Bordeaux, France) (28).

Generation of Anti-Pma1p Antisera—To generate antibodies against Pma1p, plasma membranes were isolated from wild-type cells by fractionation over a sucrose density gradient (29). Plasma membrane proteins were then separated by SDS-PAGE, and the region corresponding to Pma1p was excised and used to immunize rabbits provided and maintained by Eurogentec (Seraing, Belgium).

Pulse-chase Analysis—For pulse-chase analysis, cells were grown to A_{600} = ~1 in minimal media lacking cysteine and methionine; unless otherwise noted the culture was then split and pre-incubated at either 24 °C or 37 °C for 15 min. Cells were pulsed with 100 μCi/ml EXPRE^{35}S^{35}S protein labeling mix (~1175 Ci/mmol; PerkinElmer Life Sciences) for 5 min. Chase was initiated by addition of chase solution (100×; 0.3% cysteine, 0.3% methionine, 300 mM ammonium sulfate). At each time point, 5 A_{600} units of cells were removed, placed on ice, and arrested with 20 mM NaN_3/NaF. Cells were centrifuged; resuspended in 50 mM Tris-HCl, pH 7.5, 5 mM EDTA, 10 μg/ml leupeptin A, and 10 μg/ml pepstatin; and disrupted by vortexing with glass beads. SDS was added to 1%, and the lysate was incubated at 45 °C for 10 min. The lysate was diluted by addition of 800 μl of TNET (30 mM Tris-HCl, pH 7.5, 120 mM NaCl, 5 mM EDTA, and 1% Triton X-100) and centrifuged at 15,000 × *g* for 10 min. The supernatant was incubated with anti-Pma1p antibody and protein A-Sepharose. Immunoprecipitates were analyzed by SDS-PAGE, visualized with a phosphorimager, and quantified using the Quantify One software (Bio-Rad).

Detergent resistance of newly synthesized Pma1p was examined as previously described (25, 26). Lysates of labeled cells (3–4 A_{600} equivalents) were extracted with 1% Triton X-100 for 30 min at 4 °C. Samples were centrifuged at 100,000 × *g* for 1 h. Pellets were resuspended in 1% SDS. Detergent concentrations in aliquots of total, supernatant, and pellet samples were adjusted for immunoprecipitation.

All pulse-chase analyses were performed at least two times with essentially the same results. Deviations between independent experiments were generally <10%.

Fluorescence Microscopy—In vivo localization of GFP-tagged Pma1p was performed by fluorescence microscopy using a Zeiss Axioplan 2 microscope (Carl Zeiss, Oberkochen, Germany) equipped with an AxioCam charge-coupled device camera and AxioVision 3.1 software.

Lipid Analysis—Sterol synthesis was monitored by labeling cells with 10 μCi/ml L-[methyl-^{3}H]methionine (85 Ci/mmol; American Radiolabeled Chemicals Inc., St. Louis, MO) for 2 h at 37 °C. Cells were resuspended in methanol, and non-saponifiable lipids were extracted with heptane and analyzed by thin layer chromatography on Silica Gel 60 plates (Merck) using cyclohexane:diethylether:glacial acetic acid (40:159:1, v/v/v) as solvent system. Incorporation of radiolabel into newly synthesized sterols was quantified by one-dimensional radioscanning with a Berthold Tracemaster 40 Automatic TLC-Linear Analyzer, and plates were visualized using a phosphorimager (Bio-Rad).

RESULTS

Synthesis of Inositolphosphorylceramide Is Required for Surface Delivery of Pma1p—The fact that long chain base synthesis is required for Pma1p biogenesis, together with our previous observation that Pma1p is conditionally destabilized in an *elo3*Δ/*sur4*Δ mutant, indicates that Pma1p biogenesis is lipid-dependent (5, 23, 24, 26). To examine this lipid requirement in more detail, we first examined Pma1p stability in wild-type cells treated with inhibitors of essential steps along the sphingolipid biosynthetic pathway (Fig. 1). Myriocin (20 μg/ml) was used to block long chain base synthesis, fumonisin B1 (72 μg/ml) was used to block ceramide production, and aureobasi-

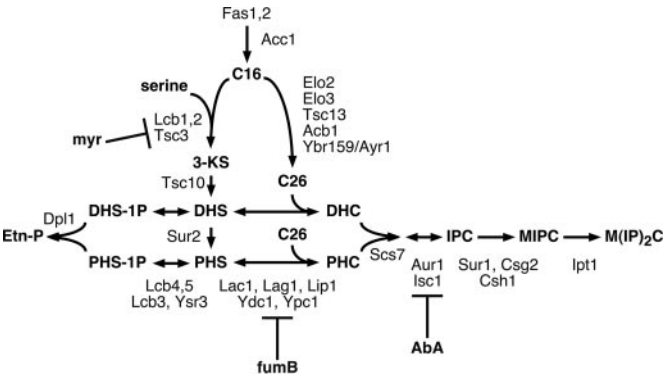

FIG. 1. **Overview of the sphingolipid biosynthetic pathway of yeast.** Schematic diagram of the sphingolipid pathway with inhibitors of essential steps, genes, and biosynthetic intermediates indicated. See the reviews cited under "Introduction" for further details. *myr*, myriocin; *fumB*, fumonisin B1; *AbA*, aureobasidin A; *3-KS*, 3-ketosphingosine; *DHS*, dihydrosphingosine; *PHS*, phytosphingosine; *DHC*, dihydroceramide; *PHC*, phytoceramide; *MIPC*, mannosyl-inositolphosphorylceramide; *M(IP)$_2$C*, mannosyl-diinositolphosphorylceramide.

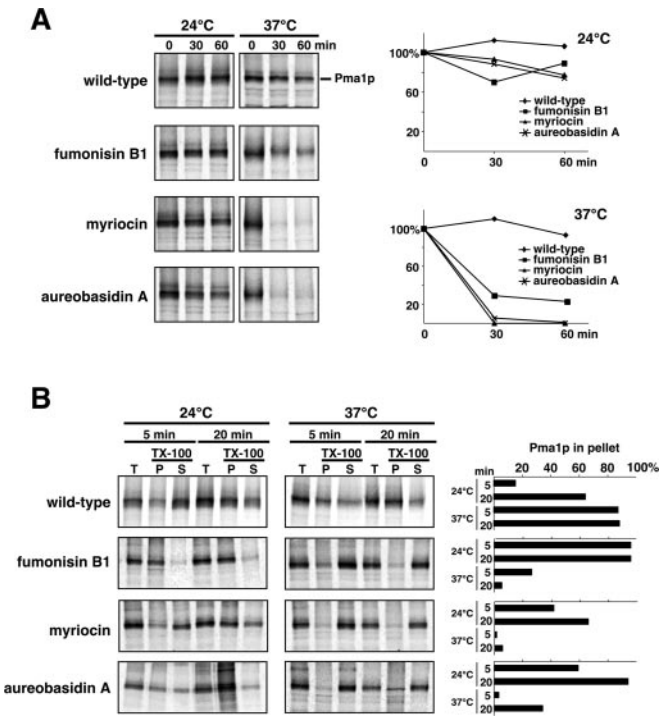

FIG. 2. **Inhibition of sphingolipid synthesis induces conditional turnover of newly synthesized Pma1p.** *A*, wild-type cells (BY4742) were cultivated in media lacking methionine and cysteine at 24 °C. Cells were incubated with myriocin (20 μg/ml), fumonisin B (72 μg/ml), or aureobasidin A (2 μg/ml) for 15 min at 24 °C, split, and incubated in the presence of drugs at either 24 °C or 37 °C prior to pulse-chase analysis and immunoprecipitation. Quantification of Pma1p levels is shown in the *graphs*. *B*, *PEP4* mutant cells (YRS1546) were incubated with the indicated drugs at 24 °C for 15 min, shifted to 37 °C for 15 min, and pulse-labeled. Samples were removed at the indicated time points after chase addition and split into a total fraction (*T*) and a fraction that was extracted with 1% Triton X-100 for 30 min on ice. The detergent fraction was centrifuged at 100,000 × *g* for 1 h to yield a detergent-resistant pellet (*P*) and a soluble (*S*) fraction. Pma1p was immunoprecipitated and analyzed by gel electrophoresis. Quantification of Pma1p levels in the detergent-resistant pellet as a function of temperature and time is shown in the *graphs*. The data shown in *A* and *B* represent one of two independent experiments with essentially the same results.

din A (2 μg/ml) was used to inhibit the conversion of ceramide to inositolphosphorylceramide (IPC) (30–32). Cells were pre-incubated with each of these drugs for 15 min at 24 °C, split, incubated at either 24 °C or 37 °C for 15 min, and pulse-labeled with [^{35}S]methionine and [^{35}S]cysteine for 5 min in the presence of the drugs. The stability of newly synthesized Pma1p was then monitored 0, 30, and 60 min after the addition of unlabeled chase solution. This analysis revealed that Pma1p is degraded in cells treated with each one of these inhibitors, indicating that sphingolipid synthesis up to IPC is required for stable production of Pma1p. The shift to 37 °C for 15 min was included to replicate the conditions under which Pma1p is degraded in *elo3*Δ mutants, and under the experimental regime used here, the temperature shift was required to destabilize Pma1p (Fig. 2*A*) (26). The temperature dependence of drug action was not limited by the time of drug pre-incubation because even 1 h of drug pre-treatment did not result in any significant destabilization of newly synthesized Pma1p when cells remained at 24 °C (data not shown).

lcb1-100 and *elo3*Δ affect detergent solubility of newly synthesized Pma1p (5, 23, 26). *lcb1-100* encodes a temperature-sensitive subunit of the serine palmitoyl transferase and can be employed to conditionally block long chain base synthesis (33). To determine whether a block in sphingolipid biosynthesis also affects detergent solubility of newly synthesized Pma1p, the fate of Pma1p was examined in *pep4*Δ mutant cells, which lack a major vacuolar hydrolase and thus fail to degrade Pma1p that has been mistargeted to the vacuole. Cells were treated with inhibitors of sphingolipid synthesis and pulse-labeled at either 24 °C or 37 °C, and the membrane pellets were extracted with cold Triton X-100 to generate detergent-soluble and detergent-resistant pellet fractions. Pma1p was then immunoprecipitated from these fractions, and the proportion of Pma1p was compared with a non-detergent-treated control (total). This analysis revealed that in wild-type cells, a large proportion (>50%) of newly synthesized Pma1p already becomes detergent-resistant at 5 min after pulse-labeling, and this pool of Pma1p further increases over time (Fig. 2*B*). In cells treated with the inhibitors and pulse-labeled at 37 °C, however, the majority of newly synthesized Pma1p was present in the detergent-soluble fraction at the 5 min time point, and only a small increase in the proportion of Pma1p that resisted detergent extraction was observed over time. This loss of detergent resistance was temperature-dependent because it was not observed when cells were labeled and chased at 24 °C. Taken together, the results of this analysis indicate that drug-induced mistargeting of newly synthesized Pma1p is temperature-dependent and correlates with the failure of Pma1p to acquire detergent resistance. The pharmacological block in sphingolipid synthesis thus results in the same conditional phenotype as previously observed in an *elo3*Δ mutant (26).

Defects or a Block in Sterol Synthesis Does Not Affect Pma1p Biogenesis—Sphingolipids associate with sterols to form membrane domains that resist detergent extraction (34). To test whether synthesis of the fungal sterol, ergosterol, is important for Pma1p biogenesis and acquisition of detergent resistance, the stability of newly synthesized Pma1p was examined in viable mutants in the post-squalene part of the ergosterol biosynthetic pathway (35). Pulse-chase analysis revealed that Pma1p was stable in all *erg* mutants tested (*erg24*Δ, *erg3*Δ, *erg4*Δ, *erg5*Δ) (Fig. 3*A*). To determine whether a block in ergosterol biosynthesis as imposed by terbinafine, an inhibitor of the fungal squalene epoxidase (36), affects Pma1p biogenesis, cells that lack endogenous steryl esters due to mutations in the two steryl ester synthetases, *ARE1* and *ARE2* (37), were treated with terbinafine (30 μg/ml) for different periods of time, and turnover of Pma1p was examined by pulse-chase labeling and immunoprecipitation. *are1*Δ *are2*Δ double mutant cells were employed to prevent the rapid replenishment of a depleted

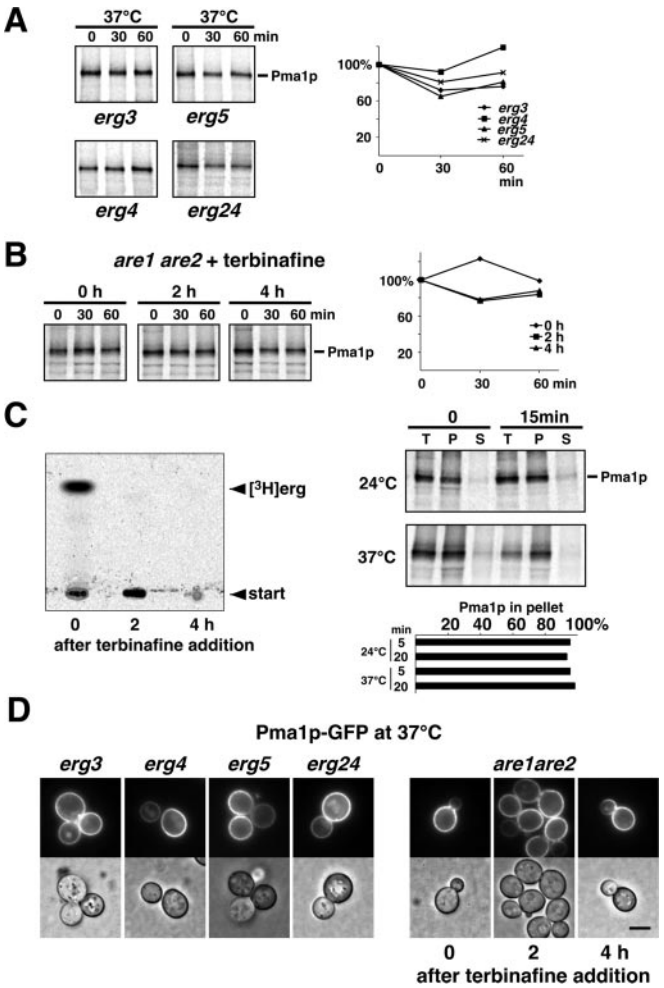

FIG. 3. **Sterol requirement for Pma1p stability.** *A*, mutations in the ergosterol biosynthetic pathway do not affect the biogenesis of Pma1p. Mutants at different steps of the ergosterol pathway (*erg3*Δ, *erg4*Δ, *erg5*Δ, and *erg24*Δ) were cultivated at 24 °C, shifted to 37 °C for 15 min, and radiolabeled, and Pma1p stability was analyzed by immunoprecipitation and quantified using a phosphorimager. *B*, inhibition of sterol biosynthesis does not affect the biogenesis of Pma1p. Cells lacking steryl esters (*are1*Δ *are2*Δ, and RSY1825) were cultivated at 24 °C, treated with terbinafine (30 μg/ml) for the time indicated, and shifted to 37 °C for 15 min in the presence of the drug, and the stability of newly synthesized Pma1p was examined by pulse-chase analysis. *C*, terbinafine efficiently blocks *de novo* synthesis of ergosterol without affecting the stability of Pma1p. *are1*Δ *are2*Δ double mutant cells were incubated with terbinafine for the time indicated and labeled with [^{3}H]methionine (10 μCi/ml) for 2 h, and lipids were extracted, saponified, and analyzed by thin layer chromatography. *are1*Δ *are2*Δ double mutant cells were incubated with terbinafine for 4 h, and detergent resistance of newly synthesized Pma1p was analyzed and quantified as described in Fig. 2*B*. The data shown in *A*–*C* represent one of two independent experiments with essentially the same results. *D*, subcellular localization of Pma1p-GFP in sterol mutants. Ergosterol biosynthetic mutants of the indicated genotype expressing Pma1p-GFP were shifted to 37 °C for 2 h and analyzed by fluorescence microscopy. *are1*Δ *are2*Δ double mutant cells expressing Pma1p-GFP were incubated with terbinafine for the time indicated and analyzed by fluorescence microscopy. *Bar*, 5 μm.

ergosterol pool by steryl ester hydrolysis (38). Remarkably, Pma1p stability was unaffected in cells treated with terbinafine for up to 4 h prior to pulse-chase labeling (Fig. 3*B*). Under these conditions, endogenous synthesis of ergosterol is completely blocked, as determined by labeling cells with [^{3}H]methionine and the analysis of radiolabeled ergosterol (Fig. 3*C*). Pulse-chase analysis followed by detergent extraction revealed that Pma1p acquired detergent resistance even in cells that were blocked in ergosterol synthesis (Fig. 3*C*). To examine whether Pma1p synthesized under these conditions is indeed

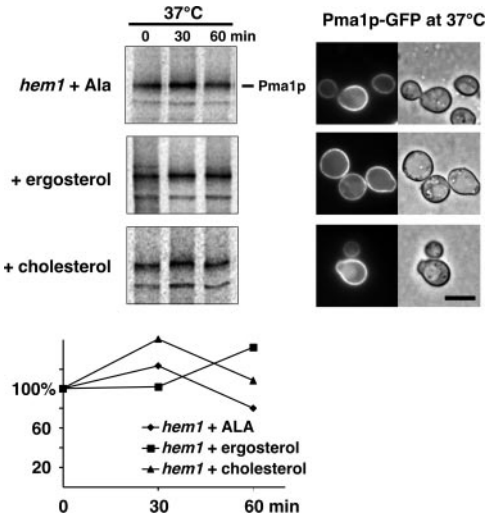

FIG. 4. **ER synthesized ergosterol is not required for Pma1p biogenesis.** *hem1*Δ mutant cells (YRS1707) were grown in media containing either ALA, ergosterol, or cholesterol for more than 48 h, and the stability of newly synthesized Pma1p was examined by pulse-chase analysis. Quantification of Pma1p levels is shown in the *graph*. The data shown represent one of two independent experiments with essentially the same results. The subcellular localization of Pma1p-GFP in *hem1*Δ mutant cells cultivated in the presence of ALA, ergosterol, or cholesterol was examined by fluorescence microscopy. *Bar*, 5 μm.

transported to the cell surface rather than accumulated in an intracellular location, we examined the subcellular distribution of a GFP-tagged version of Pma1p. *erg* mutants expressing Pma1p-GFP were cultivated for 2 h at 37 °C and then analyzed by fluorescence microscopy. Pma1p-GFP exhibited prominent ring-like staining at the cell periphery, indicative of its plasma membrane localization. Only faint staining of vacuolar structures was occasionally observed (Fig. 3*D*). *are1*Δ *are2*Δ double mutant cells expressing Pma1p-GFP were treated with terbinafine for various time periods and examined by fluorescence microscopy. Again, only ring staining of the plasma membrane was observed, indicating that the stable biogenesis of Pma1p observed by pulse-chase analysis is indicative of cell surface transport rather than due to intracellular accumulation of the protein. Taken together, these results indicate that sphingolipid synthesis up to IPC, but not the structure or even synthesis of ergosterol, is important for Pma1p to acquire detergent resistance and to be sorted to the cell surface.

ER Synthesis of Ergosterol Is Dispensable for Surface Delivery of Pma1p—Because a terbinafine-induced block inhibits *de novo* synthesis of ergosterol but does not affect the pool of pre-existing ergosterol, we examined a possible role of ergosterol in surface delivery of Pma1p using *hem1*Δ mutant cells. Heme deficiency effectively mimics anaerobic conditions and renders yeast auxotroph for sterols and unsaturated fatty acids because their synthesis requires molecular oxygen (39, 40). Hem1p catalyzes the first step in heme biosynthesis, the conversion of glycine and succinyl-CoA to ALA (39). Deficiency in *HEM1* can thus be overcome by supplementing cells with sterols and unsaturated fatty acids, thereby mimicking anaerobic conditions; alternatively, the biosynthetic block can be bypassed by providing cells with ALA, thereby allowing heme biosynthesis. To examine Pma1p stability in cells lacking the capacity to synthesize their own ergosterol, *hem1*Δ mutant cells were cultivated in the presence either of ALA, ergosterol, or cholesterol, and the stability of Pma1p was determined by pulse-chase labeling and immunoprecipitation. This analysis revealed that newly synthesized Pma1p remained stable in the heme mutant cells even when cells were grown in the presence of cholesterol over many generations (Fig. 4). Examination of

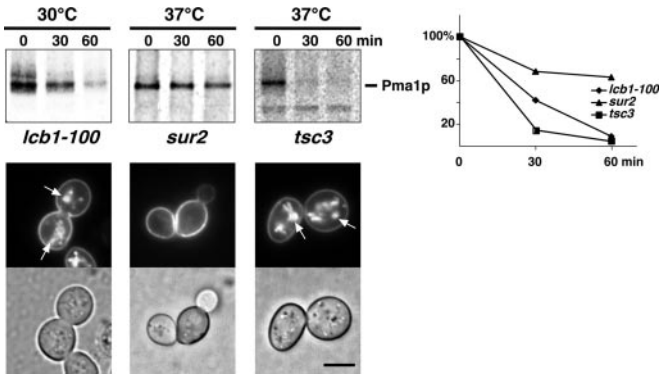

FIG. 5. **Sphingolipid requirement for Pma1p stability.** Biogenesis of Pma1p was examined in cells with defects at early steps along the sphingolipid pathway. *lcb1-100*, *sur2*Δ, and *tsc3*Δ mutant cells were cultivated at 24 °C and shifted to 30 °C or 37 °C for 15 min, and Pma1p stability was examined by pulse-chase analysis and immunoprecipitation. Levels of Pma1p were quantified using a phosphorimager. The data shown represent one of two independent experiments with essentially the same results. The subcellular localization of Pma1p-GFP in *lcb1-100*, *sur2*Δ, and *tsc3*Δ was examined by fluorescence microscopy. *Arrows* indicate localization of Pma1p-GFP in multi-lobed vacuoles. *Bar*, 5 μm.

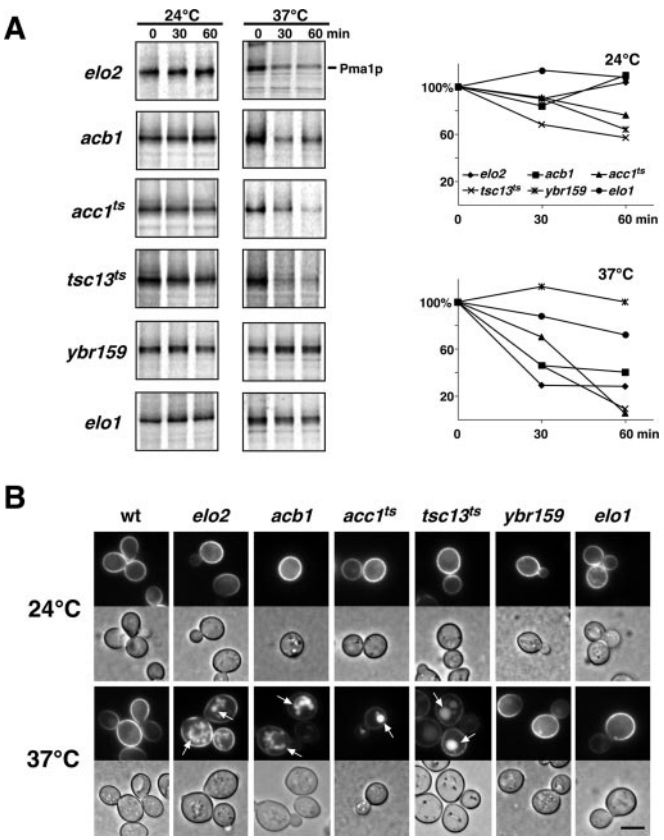

FIG. 6. **Acyl chain elongation is required for Pma1p stability.** *A*, biogenesis of Pma1p was examined in mutants that affect acyl chain elongation. Cells with the indicated genotype were cultivated at 24 °C, split, and incubated at either 24 °C or 37 °C for 15 min prior to pulse-labeling and immunoprecipitation. Levels of Pma1p were quantified using a phosphorimager. The data shown represent one of two independent experiments with essentially the same results. *B*, the subcellular localization of Pma1p-GFP in the elongation mutants was examined by fluorescence microscopy. Cells of the indicated genotype expressing Pma1p-GFP were cultivated at 24 °C, split, and incubated at either 24 °C or 37 °C for 2 h before microscopic examination. *Arrows* indicate localization of Pma1p-GFP in vacuoles. *Bar*, 5 μm.

the intracellular distribution of Pma1p-GFP under these conditions revealed surface staining, indicating that Pma1p is transported to the plasma membrane. These results thus reinforce the notion that endogenously synthesized ergosterol is dispensable for Pma1p biogenesis, indicating that sorting of Pma1p is clearly distinct from the "raft-dependent" sorting of other polytopic plasma membrane proteins, such as that of the tryptophan permease (2).

Sphingolipid Head Group Maturation and Hydroxylation Are Dispensable for Surface Delivery of Pma1p—To further define the sphingolipid requirement for Pma1p biogenesis, we examined Pma1p turnover in a large number of mutants that affect defined steps along the sphingolipid biosynthetic pathway (for review, see Refs. 15–17). These mutants can be grouped according to the step at which they affect sphingolipid synthesis (see Fig. 1). There are mutations that affect long chain base synthesis (*lcb1-100* and *tsc3*Δ), long chain base phosphorylation (*lcb4*Δ and *lcb5*Δ), dephosphorylation (*lcb3*Δ and *ysr3*Δ) and degradation (*dpl1*Δ), hydroxylation of the long chain base (*sur2*Δ) or the C26 fatty acid (*scs7*Δ), ceramide synthesis (*lac1*Δ and *lag1*Δ) and degradation (*ydc1*Δ and *ypc1*Δ), degradation of IPC (*isc1*Δ), head group maturation of IPC to mannosyl-inositolphosphorylceramide (*sur1*Δ and *csg2*Δ), and maturation of mannosyl-inositolphosphorylceramide to mannosyl-diinositolphosphorylceramide (*ipt1*Δ). With the exception of *lcb1-100* and *tsc3*Δ, none of the tested mutants displayed an increased turnover of Pma1p (Fig. 5) (data not shown). Examination of Pma1p-GFP in these mutants revealed surface staining in all of the mutants, except *lcb1-100* and *tsc3*Δ, indicating that the newly made Pma1p is not only stable but also transported to the cell surface (Fig. 5) (data not shown). These results are consistent with previous observations that *lcb1-100* affects Pma1p turnover (5, 23, 24) and that defects in mannosyl-inositolphosphorylceramide synthesis do not affect Pma1p sorting from the late Golgi apparatus (41). Moreover, they suggest that sphingolipid synthesis up to IPC, but no specific structural feature on the sphingolipid molecule, is critically important for Pma1p biogenesis.

Acyl Chain Elongation Is Required for Pma1p Biogenesis—Next, we tested whether mutations that affect the synthesis of the ceramide-bound C26 fatty acid interfere with Pma1p biogenesis. Mutations in components of the elongase complex result in lower levels of the mature C26 fatty acid rather than in a defined shortening of the very long chain fatty acid, as is the case in *elo3*Δ (18, 19, 21, 22). Analysis of Pma1p in these elongation mutants revealed a temperature-dependent destabilization of Pma1p and vacuolar localization of Pma1p-GFP in *elo2*Δ/*fen1*Δ, *acb1*Δ, *acc1*^{ts}, and *tsc13*^{ts} (18, 19, 21, 22) (Fig. 6). These results indicate that it is not only the length of the very long acyl chains but also their levels that are critically important for biogenesis of Pma1p. *YBR159* encodes a major 3-ketoreductase of the fatty acid elongase, but its function is redundant with that of another ketoreductase, Ayr1p (20). Because very long chain fatty acid synthesis is essential, the redundancy between *YBR159* and *AYR1* is likely to account for the viability of a *ybr159*Δ mutant and may also explain why this mutant does not affect turnover of Pma1p. A defect in *ELO1*, which is required for elongation of C14 fatty acids to C16/C18 fatty acids (42, 43), also affects Pma1p stability, but degradation of Pma1p is much slower compared with mutants that affect elongation to C26. Whether destabilization of Pma1p in the *elo1*Δ mutant is due to possible indirect effects of a lack of Elo1p on the synthesis of C26 remains to be established. However, the observation that rapid destabilization and vacuolar localization of Pma1p is observed only if elongation to C26 but not to C16/C18 fatty acids is impaired indicates that C26 synthesis has a more specific role in Pma1p biogenesis.

Elongase Mutants Affect Detergent Resistance of Newly Synthesized Pma1p—To determine whether the acyl chain elon-

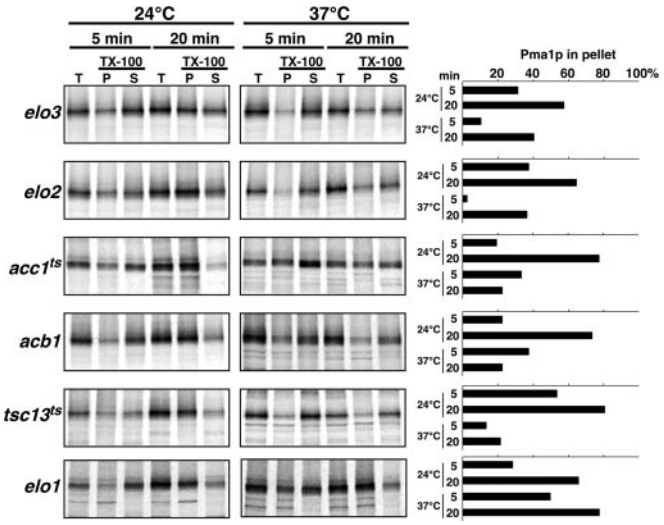

FIG. 7. **Elongase mutants affect detergent extractability of newly synthesized Pma1p.** Cells of the indicated genotype were pulse-labeled at either 24 °C or after a pre-shift to 37 °C for 15 min. Samples were removed at the indicated time points after chase addition and split into a total fraction (*T*) and a second fraction that was extracted with 1% Triton X-100 for 30 min on ice. The detergent fraction was centrifuged at 100,000 × *g* for 1 h to yield a detergent-resistant pellet (*P*) and a detergent-soluble fraction (*S*). Pma1p was immunoprecipitated and analyzed by gel electrophoresis. Quantification of Pma1p levels in the detergent-resistant pellet as a function of temperature and time is shown in the *graphs*. The data shown represent one of two independent experiments with essentially the same results.

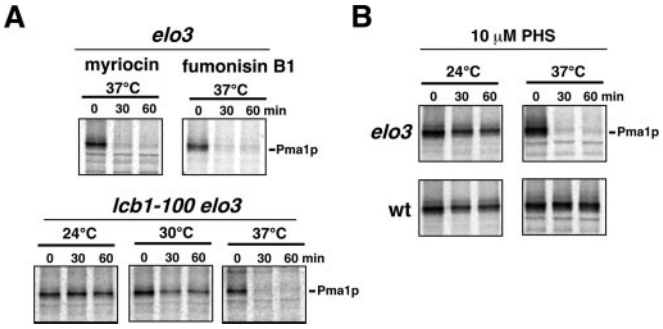

FIG. 8. **Long chain base signaling does not account for Pma1p turnover in *elo3*Δ.** *A*, a block in long chain base or ceramide synthesis fails to stabilize Pma1p in the elongase mutant. *elo3*Δ mutant cells were cultivated at 24 °C, pre-incubated with either myriocin (20 μg/ml) or fumonisin B1 (75 μg/ml) for 15 min, and then shifted to 37 °C for 15 min. *lcb1-100 elo3*Δ double mutant cells (YRS1986) were cultivated at 24 °C, split, and incubated at 24 °C, 30 °C, or 37 °C for 15 min. Cells were labeled, and Pma1p turnover was examined by immunoprecipitation. *B*, long chain base (*PHS*, phytosphingosine) addition does not stabilize Pma1p in *elo3*Δ. Wild-type and *elo3*Δ mutant cells were cultivated at 24 °C, incubated with phytosphingosine (10 μM) for 2 h, and either left at 24 °C or shifted to 37 °C for 15 min prior to labeling and immunoprecipitation of Pma1p. The data shown represent one of two independent experiments with essentially the same results.

gase mutants *elo2*Δ, *acb1*Δ, *acc1*^{ts}, and *tsc13*^{ts}, which conditionally destabilize Pma1p, also affect detergent solubility of Pma1p, the mutants were deleted for *PEP4* to prevent degradation of mistargeted Pma1p in the vacuole. Cells were then pulse-labeled at either 24 °C or 37 °C, and the detergent solubility of newly synthesized Pma1p was examined as described for Fig. 2*B*. This analysis revealed that Pma1p rapidly acquired detergent resistance in the elongase mutants when cells were pulse-labeled at 24 °C (Fig. 7). At 37 °C, however, the majority of newly synthesized Pma1p was present in the detergent-soluble fraction at the 5 min time point, and only a small increase in the proportion of Pma1p that resisted detergent extraction was observed over time. These results indicate that all the elongase mutants that conditionally affect the stability of newly synthesized Pma1p also affect its detergent resistance. The fact that a mutation in *ELO1* did not affect detergent solubility of Pma1p is consistent with the slow turnover of Pma1p observed in this mutant.

The Role of Long Chain Base and Ceramide Signaling in Pma1p Turnover—Elongase mutants have previously been shown to contain elevated levels of long chain bases and reduced levels of ceramide, both of which are potential signaling molecules (18, 19, 44–46). To test whether destabilization of Pma1p is due to a defect in lipid signaling rather than an aberrant membrane structure, we examined Pma1p stability under conditions in which long chain base or ceramide synthesis was inhibited by genetic and pharmacological means. Therefore, Pma1p turnover was examined in *elo3*Δ mutant cells treated with myriocin (20 μg/ml) to block long chain base synthesis and in *elo3*Δ treated with fumonisin B1 (75 μg/ml) to inhibit ceramide production. Inhibition of long chain base or ceramide synthesis failed to stabilize Pma1p, indicating that elevated long chain base or ceramide levels do not account for the increased turnover of Pma1p (Fig. 8*A*). To corroborate these results, a mutant with chronically low levels of ceramide, *lcb1-100*, was combined with a mutation in *ELO3*. In the resulting *lcb1-100 elo3*Δ double mutant, newly synthesized Pma1p was stable at 24 °C but destabilized at 30 °C and 37 °C, as observed in an *lcb1-100* mutant alone (Fig. 8*A*). Thus, no synthetic alleviation or enhancement of the phenotype of either single mutant was observed in the double mutant. These results are in agreement with the proposal that the conditional turnover of Pma1p in elongase mutant cells is not due to a defect in long chain base or ceramide signaling but may be due to reduced levels and/or the aberrant structure of ceramides made in these cells.

Increased levels of long chain base induce the degradation of cell surface permeases (44, 47, 48). Exogenously added long chain base (10 μM), however, did not induce increased turnover of newly synthesized Pma1p in wild-type cells at either 24 °C or 37 °C. Similarly, exogenously added long chain base failed to rescue the increased turnover of Pma1p in *elo3*Δ mutant cells and did not substitute for heat treatment (37 °C), which is known to increase long chain base levels (49, 50) (Fig. 8*B*). These results thus suggest that the increased turnover of newly synthesized Pma1p in the elongase mutant is distinct from the long chain base-induced degradation of cell surface permeases and that mistargeting of Pma1p is not due to a long chain base- or ceramide-mediated signaling event.

DISCUSSION

In this study, we have characterized the lipid requirements for surface delivery and stabilization of a newly synthesized integral plasma membrane protein, Pma1p. The results of our analyses indicate that synthesis of sphingolipids up to IPC and acyl chain elongation are critically important for Pma1p biogenesis. A block in ergosterol synthesis or defects along the ergosterol biosynthetic pathway that result in the formation of aberrant sterols, on the other hand, do not affect Pma1p biogenesis or its association with detergent-resistant membranes. Even the complete substitution of endogenously synthesized ergosterol by exogenously supplied cholesterol did not affect Pma1p biogenesis. These results thus indicate that sterols are less important for surface transport of Pma1p. Remarkably, various defects in nonessential pathways of phospholipid synthesis as imposed by mutations in *CHO1* (required for the synthesis of phosphatidylserine), in both *PEM1* and *PEM2* (required for the methylation of phosphatidylethanolamine to phosphatidylcholine) or in *PSD1* and *PSD2* (required for the decarboxylation of phosphatidylserine to phosphatidylethanol-

amine) did not destabilize Pma1p.[2] The sphingolipid requirement for Pma1p biogenesis thus appears to be rather specific and cannot be explained by a more general defect in membrane structure.

The examination of the sphingolipid requirement for Pma1p biogenesis using drugs that block essential steps or mutations in nonessential or redundant steps along the sphingolipid biosynthetic pathway revealed some of the characteristics of this lipid requirement.

(i) Inhibition of the synthesis of either long chain base, ceramide, or IPC results in conditional turnover of Pma1p, suggesting that flux through the pathway up to IPC is required for proper biogenesis of Pma1p. A block in long chain base, ceramide, and IPC biosynthesis, on the other hand, may induce Pma1p turnover indirectly, for example, through accumulation of the respective biosynthetic precursors, long chain base, ceramide, or the free very long chain fatty acids. Such indirect effects have been suggested to account for the lethality of a defect in IPC synthesis, which becomes dispensable under conditions in which ceramide does not accumulate to toxic levels (10).

(ii) The observation that mutations that block sphingolipid hydroxylation or head group maturation do not affect Pma1p biogenesis indicates that the potential of these lipid modifications to engage in hydrogen bonds is not critical for Pma1p stability (51).

(iii) All mutations that affect fatty acid elongation and the synthesis of the ceramide-bound C26 fatty acid conditionally destabilize newly synthesized Pma1p. Defects in acyl chain elongation may affect sphingolipid metabolism in at least three ways. First, elongase mutants have reduced levels of ceramide, most likely because the mature C26 fatty acid is the preferred substrate for the ceramide synthase (44, 52). Second, a reduced efficacy of the ceramide synthase results in the accumulation of long chain base (18). Third, the ceramide synthesized in elongase mutants has a shorter acyl chain (19, 26). Any one or all of these factors could account for the increased turnover of newly synthesized Pma1p. Evidence indicates that accumulation of long chain base does not account for the increased turnover of Pma1p. For example, myriocin, by itself, induces Pma1p turnover in wild-type cells but fails to rescue Pma1p when applied to *elo3*Δ mutant cells. Correspondingly, an *lcb1-100 elo3*Δ double mutant still exhibits aberrant Pma1p turnover, and no synergistic effect of the two mutations on the stability of Pma1p at either 24 °C or 30 °C is observed. In addition, exogenously added long chain base does not induce Pma1p turnover in either wild-type or *elo3*Δ mutant cells. These observations thus indicate that ceramide levels and/or their substitution with very long acyl chains is critically important for routing Pma1p to the cell surface.

Mistargeting of Pma1p is strictly temperature-dependent. Both protein folding/assembly and membrane structures are known to be particularly thermo-sensitive. Attempts to stabilize Pma1p by the use of small molecular chaperons were not successful, suggesting that aberrant protein folding may not be affected in the lipid mutant. Oligomerization of Pma1p in the ER is not critical for stability because even monomeric Pma1p is delivered to the cell surface (23). A possible additive effect of the elongation defect and the temperature treatment on membrane structure, however, is supported by the fact that mistargeting of Pma1p correlates with failure of the protein to acquire detergent solubility. Mistargeting of Pma1p may thus be due to an aberrant membrane environment. Such an aberrant membrane domain *per se* may be sufficient for redirection to the vacuole. Alternatively, the aberrant membrane environment may affect the way in which the Pma1p complex is embedded in the membrane, possibly resulting in the exposure of residues that are normally covered by the membrane. Such residues may then be recognized by certain quality control checkpoints, which are known to recognize membrane proteins with hydrophilic residues within their transmembrane domains (53).

The precise route that the newly synthesized Pma1p follows upon mistargeting to the vacuole in the elongase mutants has not yet been defined. We have previously observed that Pma1p can be stabilized in an *elo3*Δ mutant by inhibiting endocytosis from the plasma membrane (26), indicating that the protein reaches the cell surface at least transiently. Mistargeting of wild-type Pma1p in the elongase mutants, however, shares many of the characteristics observed for a temperature-sensitive mutant allele of Pma1p, Pma1-7p. Pma1-7p conditionally looses association with detergent-resistant membranes and is mistargeted to the vacuole under non-permissive conditions (24). In the case of Pma1-7p, vacuolar mistargeting occurs before fusion of Golgi-derived vesicles with the plasma membrane because a late-acting block in secretion, such as that imposed by a mutation in *SEC6* (24), fails to stabilize the mutant protein. Sorting of Pma1-7p is regulated by a Golgi-based ubiquitin-dependent quality control system because mistargeting requires an ubiquitin ligase complex containing Rsp5p, Bul1p, and Bul2p (54). Whether the same ubiquitin ligase affects mistargeting of Pam1p in the elongase mutants remains to be established.

Genetic studies provide evidence that Pma1p can reach the cell surface by multiple pathways and from within the endosomal system (55, 56). It is thus conceivable that elongase mutants affect sorting of Pma1p not from the Golgi, but from a subsequent endosomal compartment. Future studies will now be required to identify the compartment in which mis-sorting of Pma1p is sphingolipid-dependent.

Acknowledgments—We thank A. Breton, T. Dunn, and I. Hapala for reagents and A. Conzelmann for helpful discussions during the course of this study.

REFERENCES

1. Opekarova, M., Robl, I., and Tanner, W. (2002) *Biochim. Biophys. Acta* **1564,** 9–13
2. Umebayashi, K., and Nakano, A. (2003) *J. Cell Biol.* **161,** 1117–1131
3. Morsomme, P., Slayman, C. W., and Goffeau, A. (2000) *Biochim. Biophys. Acta* **1469,** 133–157
4. Ferreira, T., Mason, A. B., and Slayman, C. W. (2001) *J. Biol. Chem.* **276,** 29613–29616
5. Lee, M. C., Hamamoto, S., and Schekman, R. (2002) *J. Biol. Chem.* **277,** 22395–22401
6. Roberg, K. J., Crotwell, M., Espenshade, P., Gimeno, R., and Kaiser, C. A. (1999) *J. Cell Biol.* **145,** 659–672
7. Harsay, E., and Schekman, R. (2002) *J. Cell Biol.* **156,** 271–285
8. Gurunathan, S., David, D., and Gerst, J. E. (2002) *EMBO J.* **21,** 602–614
9. Malinska, K., Malinsky, J., Opekarova, M., and Tanner, W. (2003) *Mol. Biol. Cell* **14,** 4427–4436
10. Schorling, S., Vallee, B., Barz, W. P., Riezman, H., and Oesterhelt, D. (2001) *Mol. Biol. Cell* **12,** 3417–3427
11. Guillas, I., Kirchman, P. A., Chuard, R., Pfefferli, M., Jiang, J. C., Jazwinski, S. M., and Conzelmann, A. (2001) *EMBO J.* **20,** 2655–2665
12. Vallee, B., and Riezman, H. (2005) *EMBO J.* **24,** 730–741
13. Funato, K., and Riezman, H. (2001) *J. Cell Biol.* **155,** 949–959
14. Levine, T. P., Wiggins, C. A., and Munro, S. (2000) *Mol. Biol. Cell* **11,** 2267–2281
15. Funato, K., Vallee, B., and Riezman, H. (2002) *Biochemistry* **41,** 15105–15114
16. Dickson, R. C., and Lester, R. L. (2002) *Biochim. Biophys. Acta* **1583,** 13–25
17. Obeid, L. M., Okamoto, Y., and Mao, C. (2002) *Biochim. Biophys. Acta* **1585,** 163–171
18. Oh, C. S., Toke, D. A., Mandala, S., and Martin, C. E. (1997) *J. Biol. Chem.* **272,** 17376–17384
19. Kohlwein, S. D., Eder, S., Oh, C. S., Martin, C. E., Gable, K., Bacikova, D., and Dunn, T. (2001) *Mol. Cell. Biol.* **21,** 109–125
20. Han, G., Gable, K., Kohlwein, S. D., Beaudoin, F., Napier, J. A., and Dunn, T. M. (2002) *J. Biol. Chem.* **277,** 35440–35449
21. Gaigg, B., Neergaard, T. B., Schneiter, R., Hansen, J. K., Faergeman, N. J., Jensen, N. A., Andersen, J. R., Friis, J., Sandhoff, R., Schroder, H. D., and Knudsen, J. (2001) *Mol. Biol. Cell* **12,** 1147–1160
22. Schneiter, R., Hitomi, M., Ivessa, A. S., Fasch, E. V., Kohlwein, S. D., and

[2] B. Gaigg and R. Schneiter, unpublished data.

Tartakoff, A. M. (1996) *Mol. Cell. Biol.* **16,** 7161–7172
23. Wang, Q., and Chang, A. (2002) *Proc. Natl. Acad. Sci. U. S. A.* **99,** 12853–12858
24. Bagnat, M., Chang, A., and Simons, K. (2001) *Mol. Biol. Cell* **12,** 4129–4138
25. Gong, X., and Chang, A. (2001) *Proc. Natl. Acad. Sci. U. S. A.* **98,** 9104–9109
26. Eisenkolb, M., Zenzmaier, C., Leitner, E., and Schneiter, R. (2002) *Mol. Biol. Cell* **13,** 4414–4428
27. Winzeler, E. A., Shoemaker, D. D., Astromoff, A., Liang, H., Anderson, K., Andre, B., Bangham, R., Benito, R., Boeke, J. D., Bussey, H., Chu, A. M., Connelly, C., Davis, K., Dietrich, F., Dow, S. W., El Bakkoury, M., Foury, F., Friend, S. H., Gentalen, E., Giaever, G., Hegemann, J. H., Jones, T., Laub, M., Liao, H., Liebundguth, N., Lockhart, D. J., Lucau-Danila, A., Lussier, M., M'Rabet, N., Menard, P., Mittmann, M., Pai, C., Rebischung, C., Revuelta, J. L., Riles, L., Roberts, C. J., Ross-MacDonald, P., Scherens, B., Snyder, M., Sookhai-Mahadeo, S., Storms, R. K., Veronneau, S., Voet, M., Volckaert, G., Ward, T. R., Wysocki, R., Yen, G. S., Yu, K., Zimmermann, K., Philippsen, P., Johnston, M., and Davis, R. W. (1999) *Science* **285,** 901–906
28. Balguerie, A., Bagnat, M., Bonneu, M., Aigle, M., and Breton, A. M. (2002) *Eukaryot. Cell* **1,** 1021–1031
29. Serrano, R. (1988) *Methods Enzymol.* **157,** 533–544
30. Horvath, A., Sütterlin, C., Manning-Krieg, U., Movva, N. R., and Riezman, H. (1994) *EMBO J.* **13,** 3687–3695
31. Merrill, A. H., Jr., van Echten, G., Wang, E., and Sandhoff, K. (1993) *J. Biol. Chem.* **268,** 27299–27306
32. Nagiec, M. M., Nagiec, E. E., Baltisberger, J. A., Wells, G. B., Lester, R. L., and Dickson, R. C. (1997) *J. Biol. Chem.* **272,** 9809–9817
33. Sütterlin, C., Doering, T. L., Schimmöller, F., Schröder, S., and Riezman, H. (1997) *J. Cell Sci.* **110,** 2703–2714
34. Brown, D. A., and Rose, J. K. (1992) *Cell* **68,** 533–544
35. Lees, N. D., Bard, M., and Kirsch, D. R. (1999) *Crit. Rev. Biochem. Mol. Biol.* **34,** 33–47
36. Jandrositz, A., Turnowsky, F., and Hogenauer, G. (1991) *Gene* (*Amst.*) **107,** 155–160
37. Yang, H., Bard, M., Bruner, D. A., Gleeson, A., Deckelbaum, R. J., Aljinovic, G., Pohl, T. M., Rothstein, R., and Sturley, S. L. (1996) *Science* **272,** 1353–1356
38. Koffel, R., Tiwari, R., Falquet, L., and Schneiter, R. (2005) *Mol. Cell. Biol.* **25,** 1655–1668
39. Gollub, E. G., Liu, K. P., Dayan, J., Adlersberg, M., and Sprinson, D. B. (1977) *J. Biol. Chem.* **252,** 2846–2854
40. Lorenz, R. T., and Parks, L. W. (1991) *Lipids* **26,** 598–603
41. Lisman, Q., Pomorski, T., Vogelzangs, C., Urli-Stam, D., de Cocq van Delwijnen, W., and Holthuis, J. C. (2004) *J. Biol. Chem.* **279,** 1020–1029
42. Toke, D. A., and Martin, C. E. (1996) *J. Biol. Chem.* **271,** 18413–18422
43. Schneiter, R., Tatzer, V., Gogg, G., Leitner, E., and Kohlwein, S. D. (2000) *J. Bacteriol.* **182,** 3655–3660
44. Chung, N., Mao, C., Heitman, J., Hannun, Y. A., and Obeid, L. M. (2001) *J. Biol. Chem.* **276,** 35614–35621
45. Chung, J. H., Lester, R. L., and Dickson, R. C. (2003) *J. Biol. Chem.* **278,** 28872–28881
46. Kobayashi, S. D., and Nagiec, M. M. (2003) *Eukaryot. Cell* **2,** 284–294
47. Skrzypek, M. S., Nagiec, M. M., Lester, R. L., and Dickson, R. C. (1998) *J. Biol. Chem.* **273,** 2829–2834
48. Chung, N., Jenkins, G., Hannun, Y. A., Heitman, J., and Obeid, L. M. (2000) *J. Biol. Chem.* **275,** 17229–17232
49. Dickson, R. C., Nagiec, E. E., Skrzypek, M., Tillman, P., Wells, G. B., and Lester, R. L. (1997) *J. Biol. Chem.* **272,** 30196–30200
50. Jenkins, G. M., Richards, A., Wahl, T., Mao, C., Obeid, L., and Hannun, Y. (1997) *J. Biol. Chem.* **272,** 32566–32572
51. Simons, K., and Ikonen, E. (1997) *Nature* **387,** 569–572
52. Guillas, I., Jiang, J. C., Vionnet, C., Roubaty, C., Uldry, D., Chuard, R., Wang, J., Jazwinski, S. M., and Conzelmann, A. (2003) *J. Biol. Chem.* **278,** 37083–37091
53. Hettema, E. H., Valdez-Taubas, J., and Pelham, H. R. (2004) *EMBO J.* **23,** 1279–1288
54. Pizzirusso, M., and Chang, A. (2004) *Mol. Biol. Cell* **15,** 2401–2409
55. Luo, W. J., and Chang, A. (1997) *J. Cell Biol.* **138,** 731–746
56. Luo, W., and Chang, A. (2000) *Mol. Biol. Cell* **11,** 579–592